ELSEVIER

Polymer 43 (2002) 5299–5309

polymer

www.elsevier.com/locate/polymer

Gelation mechanism of agarose and κ-carrageenan solutions estimated in terms of concentration fluctuation

Masaru Matsuo*, Toshie Tanaka, Lin Ma

Department of Clothes and Apparel Science, Faculty of Human Life and Environment, Nara Women's University, Nara 630-8263, Japan

Received 29 October 2001; received in revised form 18 March 2002; accepted 23 April 2002

Abstract

The gelation mechanism of agarose and κ-carrageenan aqueous solutions was investigated by using polarized light scattering and X-ray diffraction techniques in terms of the liquid–liquid phase separation. When an incident beam of He–Ne gas laser was directed to the gel prepared by quenching the agarose solution, the logarithm of scattered intensity increased linearly in the initial stage and tended to deviate from this linear relationship in the latter stage. If the linear increase in the initial stage could be analyzed within the framework of the linear theory of spinodal decomposition proposed by Cahn, the phase diagram indicated that the gelation is attributed to the phase separation due to the concentration fluctuation of solution. Furthermore, in the later stage showing the deviation of the linear relationship, light scattering under Hv polarization condition showed a X-type pattern indicating the existence of optically anisotropic rods, the optical axes being parallel or perpendicular with respect to the rod axis. In spite of the existence of the rods, no crystallites were confirmed by the corresponding X-ray diffraction and DSC measurements. For κ-carrageenan solutions, the logarithm of scattered intensity against time showed a constant value. This indicated that the gelation of κ-carrageenan solutions is independent of liquid–liquid phase separation but is due to the rapid formation of cross-linking points. Accordingly it turns out that the small difference of chemical structure between agarose and κ-carrageenan causes quite different gelation mechanism.

Keywords: Gelation mechanism; Agarose; κ-carrageenan

1. Introduction

Polymer chains usually form an inter-connected network that give rise to characteristic texture and properties, in the interstice of which are molecules of solvent and other species. Of course, gel formation involves association of chain segments, resulting in a three-dimensional framework that contains solvent in the interstices. The associated regions are known as junction zones, and may be formed from two or more chains.

Recent improvements have led to a number of new insights for the investigation of ordered state of polysaccharides, since the chains can adopt a variety of ordered shapes in the condensed phase such as the various types of ribbons and helixes including double and triple helixes. Among polysaccharides, agarose and carrageenan from marine red algae have been investigated for the sol–gel inter-conversion in relation to the morphological and mechanical aspects [1–5]. Most of the investigations by using the specimens with different molecular weights have been concentrated on the aspects of food science.

Apart from a series of the investigations [1–5], Prins et al. [6,7] studied the gelation mechanism of agarose on the basis of the time dependence of scattered intensity of He–Ne gas laser from the gels prepared by quenching solutions. According to their experiment [7], the logarithm plots of the scattered intensity against time at only one fixed scattering angle showed a straight line, as has been observed for the phase separation of amorphous blend films [8]. They concluded that the initial gelation of agarose is due to the liquid–liquid phase separation associated with spinodal decomposition. Certainly, their paper for agarose [7] was the first proposal that the gelation is associated with the liquid–liquid phase separation and after then similar analysis has been reported for several kinds of polymers [9,10]. Although their investigations for agarose were only the suggestion, more systematic results to justify their concept must be needed.

Recently, the gelation of polymer solutions by quenching has been done for poly(vinylalcohol) (PVA) with intra- and inter-molecule hydrogen bonds by Kanaya et al. [9] using

* Corresponding author. Tel./fax: +81-742-20-3462.
E-mail address: m-matsuo@cc.nara-wu.ac.jp (M. Matsuo).

0032-3861/01/$ - see front matter
PII: S0032-3861(02)00290-2

wide- and small-angle neutron scattering and by Matsuo et al. [10] using X-ray diffraction, small-angle light scattering (SALS) under Hv and Vv polarization conditions and scanning electron microscopy (SEM). Following Kanaya et al. [9], cross-linking points or junction points in the gels are crystallites taking a clear boundary surfaces and the correlation length is assigned to the average distance between the neighboring crystallites. The experiments by Matsuo et al. [10] indicated that the mechanical properties of the PVA dry gel films are sensitive to morphology determined by kinds of solvents as well as quenching temperature of the solutions and interestingly the morphology of the gels and films maintain the characteristics of the phase separation of the solutions. They pointed out that the gelation is due to the liquid–liquid phase separation associated with spinodal decomposition. Namely, PVA solutions at elevated temperature are thermodynamically unstable at the gelation temperature and tend to incur phase separation. In such supercooled solutions, compact molecular aggregates may be formed and these connect to the heterogeneous network system (polymer-rich phase). The behavior did not provide the crystallization in spite of the ordering of molecules in the polymer-rich phase.

The gelation mechanism at the initial stage, however, has never been reported in accordance with the concept by spinodal decomposition. Based on the results for PVA, this paper deals with the gelation mechanism of agarose and κ-carrageenan solutions. The main focus is concentrated on the difference of gelation mechanism between both the solutions. The estimation is done by using X-ray and light scattering techniques.

2. Experimental section

Agarose and κ-carrageenan were used as test specimens. Agarose produced for the measurement of electrophoresis was purchased from Wako Junyaku Co. Ltd. The contents of sulfate and sulphur are less than 1.0 and 0.3%, respectively. The strength of gels are less than 600 g cm^{-2}. κ-Carrageenan was furnished by San-Ei Gen F.F.I. Co. Ltd. The characteristics after purification and the cation content were reported already elsewhere (see Fig. 1 and Table 1 of Ref. [11]). Distilled water (H_2O) was used as solvents for both the specimens. The solution in glass tube was prepared by heating the well-blended polymer/solvent mixture at 80 °C for 20 min under nitrogen. The sample was set in a sample holder of light scattering instrument which had been controlled at 80 °C and quenched to desired temperature. To measure time dependence of scattered intensity by using He–Ne gas laser, ten photo-diodes were set at the desired scattering angle in order to detect the scattering beam at various angles simultaneously.

To determine the gelation temperature, test tube containing the solution was tilted after standing for 5 h in a water bath at constant temperature. When the meniscus deformed but the specimen did not flow under its own weight, we judged that the solution had gelled. The lowest temperature at which the onset of gelation occurred within 5 h was defined as the gelation temperature. This is similar to the method used in the previous paper [10].

SALS under Hv polarization condition was observed with a 15 mV He–Ne gas laser as the light source. The scattered intensity was too weak to be detected by photographic film, since most of the beam could not pass through the analyzer. Therefore, the reflected pattern on the gel surface was detected by commercial camera.

The complex dynamic tensile modulus of dry gel films was measured at 10 Hz over the temperature range from − 150 to 300 °C by using a visco-elastic spectrometer (VES-F) obtained from Iwamoto Machine Co. Ltd. The length of the specimen between the jaws was 40 mm and the width was about 1.5 mm. During measurements, the specimen was subjected to a static tensile strain of 0.1% in order to place the sample in tension during the axial sinusoidal oscillation. The complex dynamic modulus was measured by imposing a small dynamic strain to ensure linear visco-elastic behavior of the specimen [12].

The X-ray measurements were carried out with a 12 kW rotating-anode X-ray generator (Rigaku RDA-rA) operated at 200 mA and 40 kV. The X-ray beam was monochromatized with a curved graphite monochrometer. Wide-angle X-ray diffraction (WAXD) patterns were obtained with a flat camera using Cu K_α radiation. Time resolution of WAXD intensity was done to study gelation mechanism by using a curved position-sensitive proportional counter (PSPC) to estimate the change in diffraction intensity distribution as a function of the Bragg angle. The sample preparation was done by the procedure similar to the light scattering measurement.

The DSC measurements were performed with an Exstar 6000 of Seiko Instrument Incorporation. The heating rate was 1 °C mm^{-1}. The weight of gel was 38 mg. In these experiments, gel was packed without any space.

3. Results and discussion

Figs. 1 and 2 show the change in the logarithm plots of the scattered intensity against time at various q observed for 1 and 2.5% agarose solutions, respectively, where the magnitude of the scattered vector, q, is given by $q = (4\pi n/\lambda)\sin(\theta/2)$, where λ, θ and n are the wavelength of light in solution, the scattering angle and the refractive index of the solvent, respectively. The logarithm of the scattered intensity, $\ln I$ increases linearly with time in the initial stage of phase separation and tends to deviate from the linear relationship. Of course, the gelation was confirmed in the initial stage. The deviation shifts to shorter time scale as temperature decreases. If the linear relationship is related to liquid–liquid phase separation, the appearance of slightly opaque agarose gel must be independent of the crystallization.

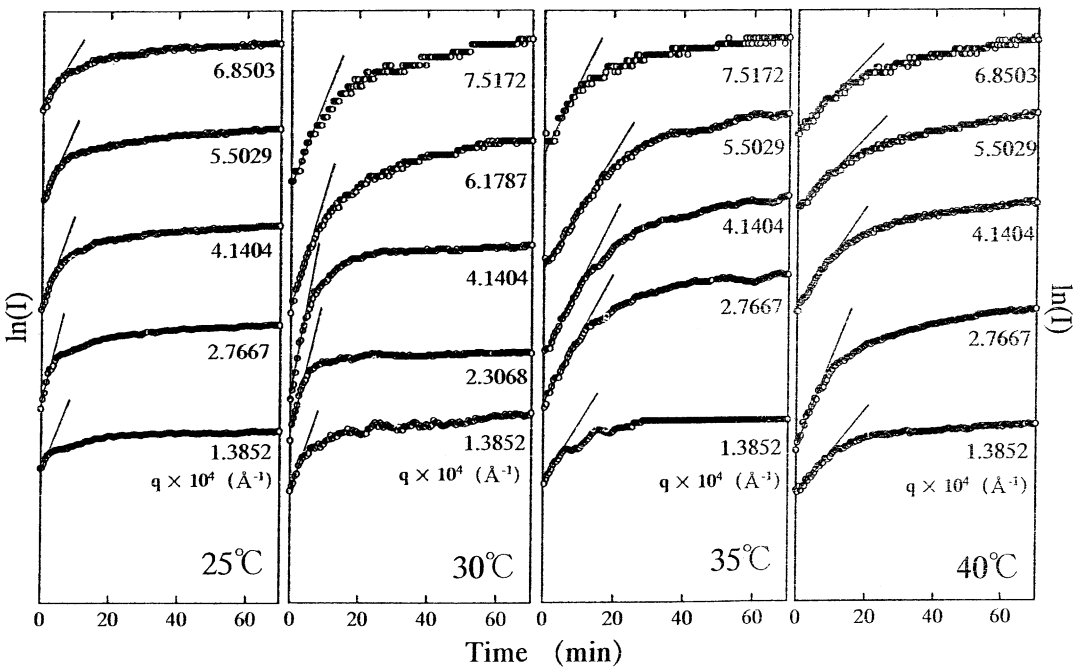

Fig. 1. Change in the logarithm plots of scattered intensity against time at various q values measured for 1.0% agarose aqueous solution at various temperatures.

To check this, SALS under Hv polarization condition and X-ray diffraction were observed.

Fig. 3 shows the change in ln I at $\theta = 15°$ and appearance of Hv pattern against time measured for 1.0 and 2.5% solutions at 30 °C. Hv scattering showed an indistinct circular type, indicating the formation of random array of quasi-crystallites smaller than the wavelength of the incident beam, in the time scale showing the straight line of ln I versus time t. With increasing time, the plots of ln I versus t deviates from the straight line and the corresponding Hv scattering shows a X-type pattern indicating the existence of optically anisotropic rod-like textures, the optical axes being oriented parallel or perpendicular to the rod axis [13]. With further lapse of time, the pattern becomes more distinct indicating the increase in the number of rods associated with the gradual development of gelation. Even so, the scattered intensity is much weaker than that from rods within crystalline polymer films as described in

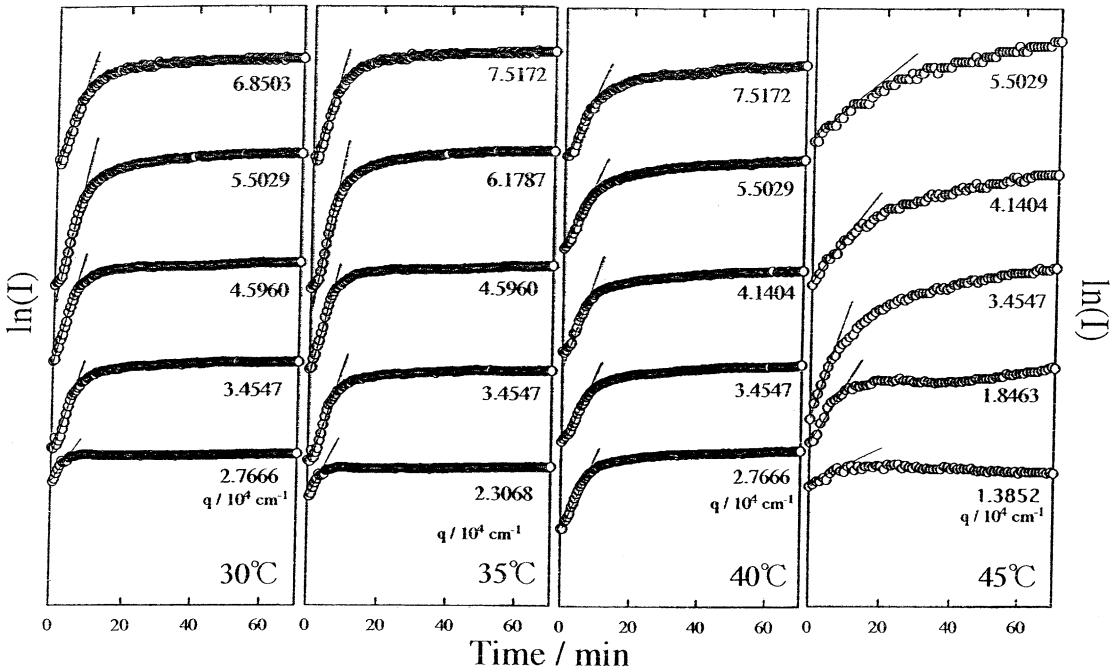

Fig. 2. Change in the logarithm plots of scattered intensity against time at various q values measured for 2% agarose aqueous solution at various temperatures.

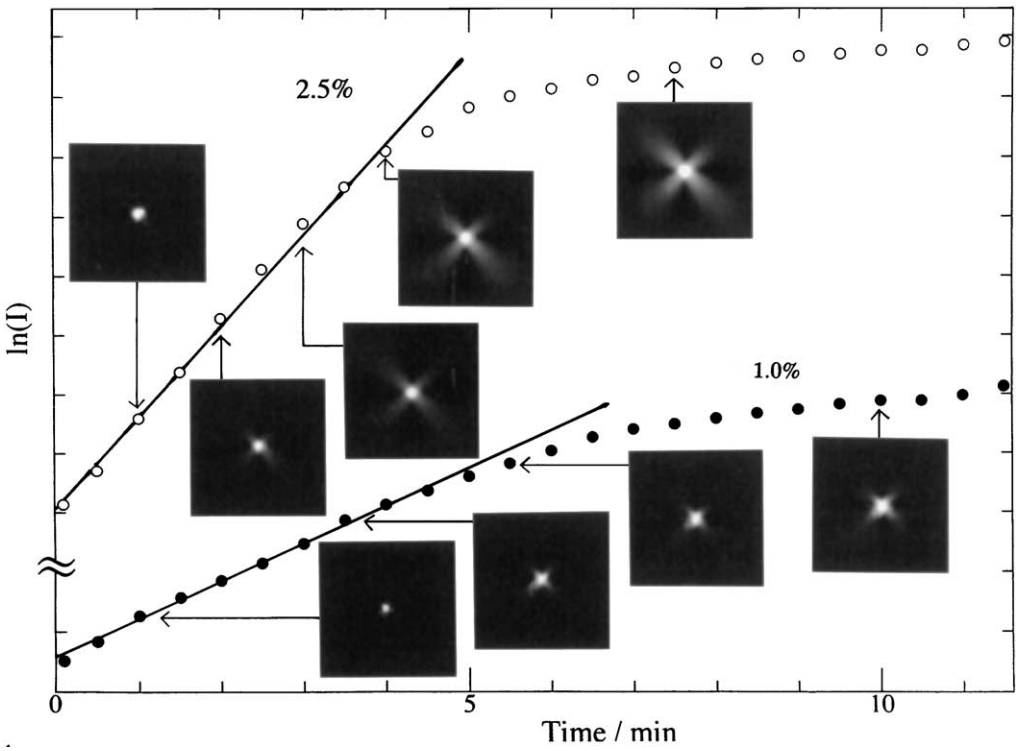

Fig. 3. Change in ln I at $\theta = 15°$ and Hv light scattering patterns with time measured for 1.0 and 2.5% agarose aqueous solutions at 30 °C.

Section 2. This is due to the small difference of optical density between rods and the medium.

A question can be arisen as to whether quasi-crystallites with crystal lattice were performed in the rods. To check this phenomenon, X-ray diffraction intensity was measured as a function of time, when the solution at 80 °C was quenched to 25 or 45 °C immediately. Fig. 4 shows the results for the 2.5% solution. The X-ray intensity shows a broad peak associated with the scattering due to the ordering of water molecules and no diffraction peak from agarose crystallites is detected. The observation reveals that the crystallization was not apparently observed even after 72 h indicating that crystallization is independent of the formation of stiff gels. The molecular ordering within the rod is too poor to derive the appearance of quasi-crystallites.

Fig. 5(a) shows the DSC curves for agarose solution with 2.5% concentration under heating and cooling processes. No peak was observed under the two processes. No endotherm peak indicates absence of crystallites in the gel. Of course, no exotherm peak indicates any chain arrangement under the melting process of the gel. Fig. 5(b) shows the DSC curves for κ-carrageenan solution with 3% concentration under heating and cooling processes. This result shall be discussed later.

Through the results in Figs. 1–5, no crystallization occurs under gelation process of agarose solutions. Accordingly, the linear increase in the logarithm of the scattered intensity against time is thought to be due to the possibility of successful analysis of the linear theory of spinodal decomposition proposed by Chan [14]. The deviation of the linear relationship is similar to the later stage of spinodal decomposition as has been observed for amorphous blends [8]. The deviation shifts to shorter time scale as the temperature decreases.

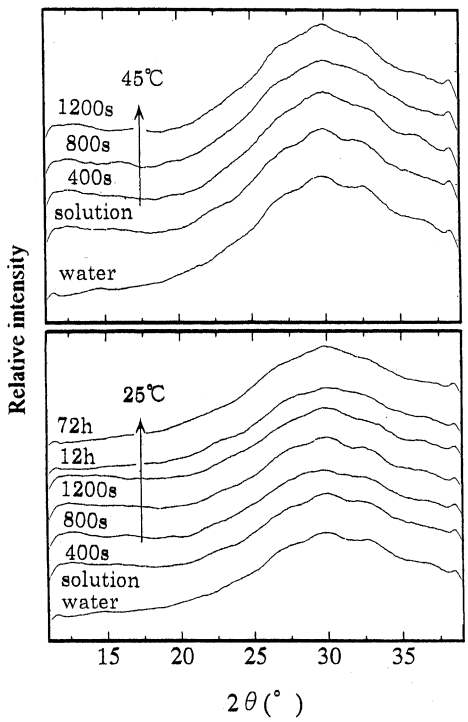

Fig. 4. Time resolved WAXD intensity distribution as a function of twice the Bragg angle from 2.5% agarose aqueous solutions after quenching at 45 °C (upper column) or 25 °C (lower column).

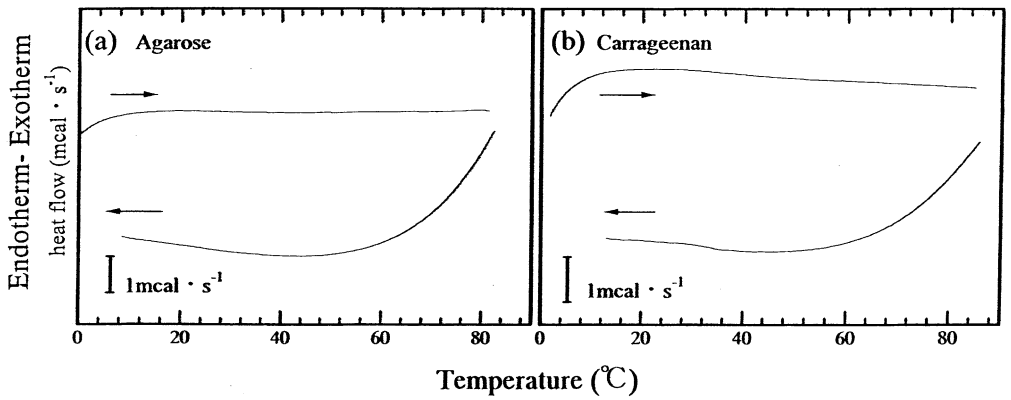

Fig. 5. DSC curves of agarose aqueous solutions (2.5%) and κ-carrageenan aqueous solutions (3%) under heating and cooling processes: (a) agarose; (b) κ-carrageenan.

If the linear relationship reflects the initial stage of spinodal decomposition as pointed by Cahn [14], it is well known that the change in scattered intensity in Figs. 1 and 2 can be given by

$$I(q,t) = I(q,t=0)\exp[2R(q)t] \quad (1)$$

where $I(q,t)$ is the scattered intensity at the time t, after initiation of the spinodal decomposition, and $R(q)$ is the growth rate of concentration fluctuation given as a function of q; $R(q)$ is given by

$$R(q) = -D_C q^2\{\partial^2 f/\partial c^2 + 2\kappa q^2\} \quad (2)$$

where D_C is the translational diffusion coefficient of the molecules in solution, f is the free energy of mixing, c is the concentration of solution, and κ is the concentration-gradient energy coefficient defined by Cahn and Hilliard [15]. A linear relationship in the plots of ln I versus t at fixed q was also confirmed up to 3% concentration.

Through a series of experimental results concerning the phase separation of agarose solutions, a question can arise as to whether or not phase separation of the solutions is always attributed to the spinodal decomposition, if the linear relationship shown in Figs. 1 and 2 can be observed. To pursue the detailed discussion, first the spinodal temperature T_S was estimated according to the linear Cahn's theory [14]. The treatment was described elsewhere [16]. The results are shown in Table 1. Incidentally, the values of $D_{app}(= D_C(\partial^2 f/\partial c^2))$, listed in Table 2, are efficiently estimated by obtaining an intercept at $q^2 = 0$ in the plot $R(q)/q^2$ versus q^2 by assuming pure spinodal decomposition. Because of the positive values of D_C by definition, the values of D_{app} are negative characterizing unstable regions, leading to spinodal decomposition. The small values of $\partial^2 R(q)/\partial q^2|_{q=q_m}$, hence $D_{app}(\partial^2 R(q)/\partial q^2|_{q=q_m} = 8D_{app})$, indicate no appearance of a scattering maximum of intensity at the initial stage of spinodal decomposition. To observe a distinct scattering maximum in the linear spinodal decomposition regime, it is evident that the value of D_{app} must be usually two or three orders of magnitude greater.

Here it is seen that the spinodal temperature, T_S, listed in Table 1, shifts to higher value as the concentration of agarose solution increases. Interestingly, the values are similar to those of poly(vinylalcohol) in dimethyl sulfoxide/water mixtures [10].

Fig. 6 shows the growth rate of concentration $R(q)$ plotted against q. The maximum growth rate $R(q_m)$ of concentration fluctuation increases with decreasing measurable temperature. The value of the scattering vector, q_m, shifts slightly towards higher value of q with increasing difference $(T_S - T)$ between the measured temperature, T, and spinodal temperature T_S. This phenomenon satisfy the principle of spinodal decomposition for amorphous polymer solutions proposed by van Aartsen [17]. According to his theory, the value of q_m increases with increasing difference $(T_S - T)$, if the range of molecular interaction associated with the mean square radius of gyration based on the concept of Debye et al. [18] is independent of temperature. Thus the shift of $R(q_m)$ to a higher value of q on increasing the difference $(T_S - T)$ justified the earlier conclusion that the linear theory of the spinodal decomposition proposed by

Table 1
Spinodal temperatures of agarose aqueous solutions

Concentration (%)	SD temperature (°C)
1.0	47.0
1.5	47.5
2.0	48.8
2.5	49.8

Table 2
Values of D_{app} ($\times 10^{-13}$ cm s^{-1}) for agarose aqueous solutions

Temperature (°C)	Concentration (%)			
	1.0	1.5	2.0	2.5
25	0.868			
30	0.610	0.723	0.745	0.815
35	0.423	0.535	0.539	0.650
40	0.224	0.341	0.395	0.440
45	0.150	0.121	0.201	0.230

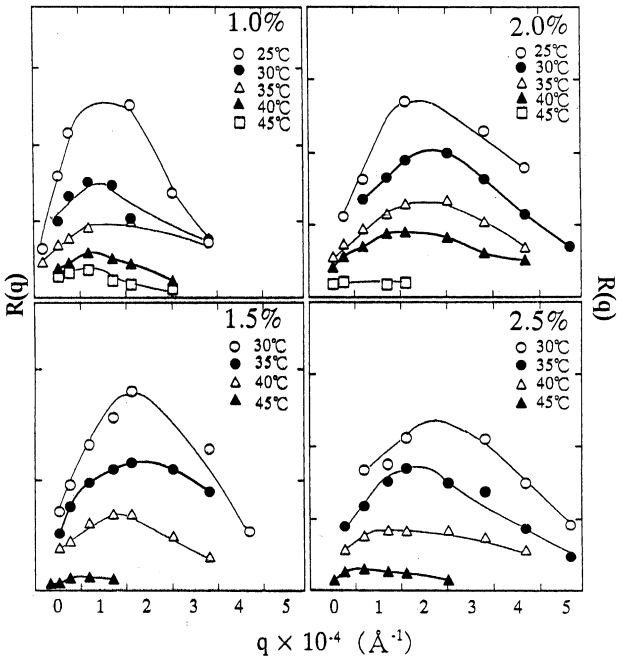

Fig. 6. Variations in growth $R(q)$ of spinodal decomposition with q measured for aqueous solutions with 1.0, 1.5, 2.0 and 2.5% concentrations at the indicated temperatures.

van Aartsen [17] and the theory of Cahn et al. [14,15] are suitable for agarose solutions. In other words, Eq. (2) associated with the linear Cahn's theory is applicable for the analysis of the linear relationship of ln I versus t in Figs. 1 and 2.

Following Cahn's theory [14,15], the concentration fluctuation relating to Eq. (1) at the proper long time t can be rewritten approximately as follows

$$\langle |C(q,t) - C_o|^2 \rangle \sim \langle |C(q_m,t) - C_o|^2 \rangle \propto \exp[2R(q_m)t] \quad (3)$$

where $|C(q,t) - C_o|$ is the concentration fluctuation at t. Eq. (3) suggests the existence of a scattering peak at θ_m from $q_m = (4\pi n/\lambda)\sin(\theta_m/2)$. Actually, the scattering peak has been observed at a later stage of spinodal decomposition for amorphous blend films [19]. No appearance of the scattering peak at the later stage of phase separation of agarose solutions is thought to be due to the very broad curve of $R(q)$ against q (Fig. 6).

Next the gelation mechanism of κ-carrageenan aqueous solutions was investigated in comparison with the gelation of agarose solutions. The difference of chemical structure between κ-carrageenan and agarose is the existence of OSO_3 groups in a pyranose ring in stead of OH groups.

Fig. 7 shows the change in the logarithm plots of the scattered intensity against time at various q observed for 3% κ-carrageenan solution. The scattered intensity shows a constant value independent of time indicating no growth rate of concentration fluctuation. The gelation does not occur beyond 40 °C. A constant value of ln I against time indicates that the rapid gelation of the solution prevents the concentration fluctuation of solution. Furthermore, no scattering pattern under Hv polarization condition was observed from transparent κ-carrageenan gels. This suggests that the gelation mechanism of κ-carrageenan gels is different from that of agarose gels. Of course, the κ-carrageenan gels do not form their crystal lattice as detected by X-ray diffraction. This is shown in Fig. 8, in which X-ray diffraction intensity at indicated time was measured as a

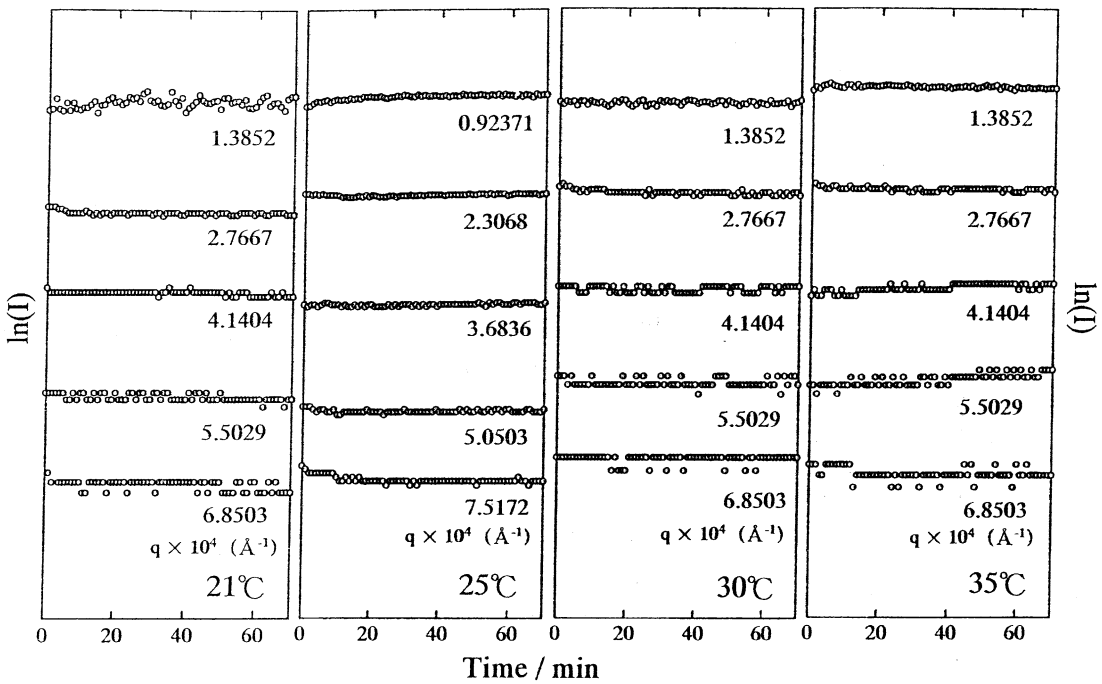

Fig. 7. Change in the logarithm plots of scattered intensity against time at various q values measured for 3.0% κ-carrageenan aqueous solution at various temperatures.

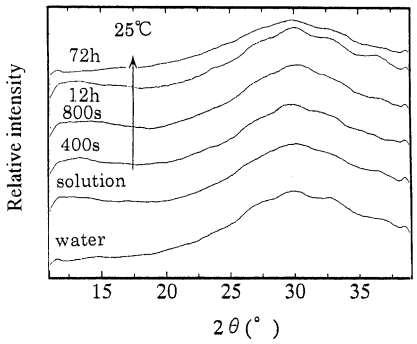

Fig. 8. Time resolved WAXD intensity distribution as a function of twice the Bragg angle from 3.0% κ-carrageenan aqueous solutions quenched at 30 °C.

function at twice the Bragg angle, when the solution at 80 °C was quenched to 25 °C immediately. As discussed for the agarose gels in Fig. 4, the X-ray intensity shows a broad peak associated with the scattering due to the ordering of water molecules and no diffraction peak from κ-carrageenan crystallites is detected. The observation reveals that the crystallization did not occur even after 72 h. This indicates that cross-linking junction points needed to form stiff gels are independent of crystallization. The same phenomenon was observed for the solution quenched to 21 °C.

Returning to Fig. 5(b), DSC curves for κ-carrageenan solution with 3% concentration show no peak under heating and cooling processes. This indicates that gelation mechanism of κ-carrageenan solutions is independent of the crystallization as well as molecular ordering by hydrogen bonds. The detailed discussion shall be done later.

Fig. 9(a) shows the phase diagram concerning the concentration dependence of spinodal temperature (T_S) and gelation temperature of agarose solutions, in which the solid curve corresponds to gelation temperature and it was

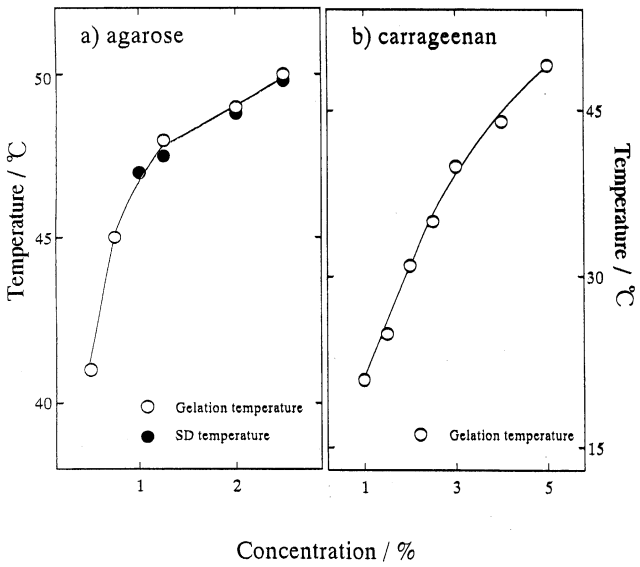

Fig. 9. Spinodal and gelation temperatures versus concentration of aqueous solutions: (a) agarose; (b) κ-carrageenan.

drawn to follow the plotted open point of gelation temperature. At temperatures above the solid curve, the sol–gel transition cannot occur, while at temperatures below the solid curve, the gelation rate becomes faster as the temperature decreases. As can be seen in Fig. 8(a), the phase diagram of agarose solutions indicates that the gelation and spinodal decomposition occur at almost same temperature. This justifies that the gelation occurs by the liquid–liquid phase separation due to concentration fluctuation, associated with spinodal decomposition. Namely, agarose solutions at elevated temperature are thermodynamically unstable at the gelation temperature and tend to incur phase separation.

Fig. 9(b) shows the concentration dependence of gelation temperature of κ-carrageenan solution. Judging from no time dependence of ln I under gelation process as shown in Fig. 7, the gelation arisen by quenching κ-carrageenan solution is thought to be not due to liquid–liquid phase separation but due to the random formation of cross-linking points in solution. No Hv scattered intensity from κ-carrageenan gels could be observed. Of course, the photographs (cross-polarized) show dark vision. This indicates no existence of rod-like texture and spherulitic texture as well as no formation of random array of quasi-crystallites smaller than the wavelength of the incident beam. In this case, the optical axes between the cross-linking points take random orientation within gels and the gels become stiffer with increasing number of cross-linking points. On the other hand, as discussed earlier, Hv scattering from agarose gels shows an indistinct circular pattern indicating random array of double helix chains smaller than the wavelength of the incident beam in the initial stage showing a linear increase in ln I against time and the progression of the aggregation by further phase separation form optically anisotropic rods.

A question can arise whether the phase diagram is useful to understand the detailed mechanism of phase separation of both the solutions. Actually, the gelation temperature was determined after keeping the solution for 5 h, while the spinodal decomposition temperature is defined in the initial stage of spinodal decomposition which corresponds to shorter time scale than 1 h as shown in Figs. 1 and 2. If the gelation was defined at such a time scale that the plots of ln I versus time starts to deviate from the linear relationship as shown in Figs. 1 and 2, the gelation temperature becomes lower than the solid curve in Fig. 9. In the case, the gelation temperature is postulated to be almost equal to the spinodal temperature indicating simultaneous advance of both gelation and spinodal decomposition.

To check the above concept, the gelation time must be estimated at temperature adopted for measuring the change in the logarithm plots of the scattered intensity against time in Figs. 1, 2, and 7. Table 3 shows the gelation time of the agarose and κ-carrageenan solutions at the indicated time. Gelation time of the agarose solution becomes shorter with increasing concentration and measured temperature.

Table 3
Gelation time (sec) at the indicated temperature measured for agarose and κ-carrageenan aqueous solutions as a function of concentration

Concentration (%)	Temperature (°C)					
	21	25	30	35	40	45
Agarose						
1.0		130	180	220	270	
2.5			120	150	220	290
κ-carrageenan						
3.0	90	120	150	210		

Judging from the linear increase of $\ln I$ against time in Figs. 1 and 2, it was confirmed that the gelation of agarose solutions occurs at the very initial stage of a time scale assuring the linear relationship but the linear relationship is slightly maintained after the gelation. Anyway, the linear relationship tends to deviate with advance of gelation. On the other hand, the constant value of $\ln I$ against time is obviously independent of the gelation time of the κ-carrageenan solutions. This satisfies the concept that the gelation of κ-carrageenan solutions is due to an increase in cross-linking junction points, independent of liquid–liquid phase separation.

Here, we must emphasize that although the X-ray curves in Figs. 4 and 8 and DSC curves in Fig. 5 indicate no crystallization under gelation processes of the agarose and κ-carrageenan solutions, these results are due to existence of quasi-crystallites with such large fluctuation of crystal lattice distance that cannot be detected by X-ray and DSC instruments. If there exists no cross-linking points, it is obvious that the physical gel cannot form. Accordingly, the quasi-crystallites must play an important role as cross-liking points to form gels.

For the agarose gels, Hv scattering shows X-type pattern at the later stage of the gelation as shown in Fig. 4. However, we must emphasize that the Hv scattered intensity I_{HV} is much weaker than the corresponding Vv scattered intensity I_{Vv} and especially the intensity of X-type lobes is extremely very weak. Of course, Vv scattering shows the circular pattern with no μ-dependence indicating isotropic scattering. In such an initial stage showing a circular type of Hv pattern, we have [20]

$$I_{Vv} - \frac{4}{3} I_{Hv} = K\langle\eta^2\rangle \int_0^\infty \gamma(r) \frac{\sin qr}{qr} \mathrm{d}r \tag{4}$$

where $\langle\eta^2\rangle$ is the mean-square polarizability fluctuation and $\gamma(r)$ is the corresponding correlation function. In the present study, the angular dependence of scattered intensity is assumed to be a monotonically decreasing function. Such a function, $\gamma(r)$, is very difficult to obtain by a Fourier transformation with sufficiently accuracy. The desired information could be extracted by assuming that the scattering over the entire angular range can be described by the sum of Gaussian functions [21]. Then we have

$$\gamma(r) = X \exp\left(-\frac{r^2}{a^2}\right) + (1 - X)\exp\left(-\frac{r^2}{b^2}\right) \tag{5}$$

Substituting Eq. (5) into Eq. (4) and performing the integration yields

$$I_{Vv} - \frac{4}{3} I_{Hv} = K\sqrt[\pi]{3}\langle\eta^2\rangle \times \left[Xa^3 \exp\left\{-\frac{a^2q^2}{4}\right\} + (1 - X)b^3 \exp\left\{-\frac{b^2q^2}{4}\right\}\right] \tag{6}$$

The parameters a and b are the correlation length estimating the extension of the inhomogeneities and the parameter X is the fraction. The gel becomes an uniform structure when a takes infinite value at $X = 1$.

Upper columns in Fig. 10 show the plots of $\ln I$ against q^2 for the agarose gel prepared by quenching 2.5% solutions at 25 °C and for κ-carrageenan gels prepared by quenching 3% solutions. The measurements were done after 5 min, ensuring a circular Hv scattering pattern (Fig. 3). The plots indicates justice of the two components shown in Eq. (5). The value of b can be obtained from the slope of straight line at wider angle and a can be estimated from the slope of the straight lines obtained after subtracting the straight line at the wider angle from $\ln I$ as shown in the lower columns. X can be estimated from Eq. (6) at $q = 0$. The values of a and b of the κ-carrageenan gel are much shorter than those of the agarose gel.

Fig. 11 shows $\gamma(r)$ curves recalculated by using the values of a, b and X. The profile of $\gamma(r)$ of the κ-carrageenan gel is much broader than that of the agarose gel, since a and

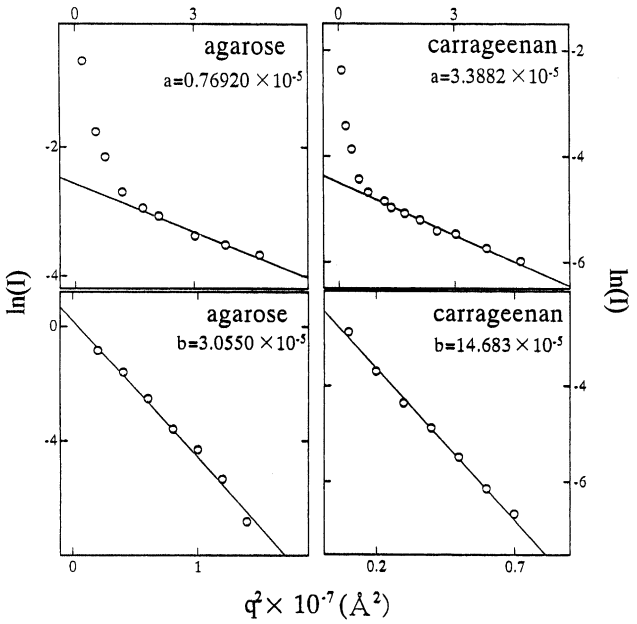

Fig. 10. Plots of $\ln I$ against q^2 for the agarose gel (2.5%) and κ-carrageenan gel (3.0%) measured at 30 °C. Two correlation distances were estimated by assuming that the plots can be classified into two straight lines.

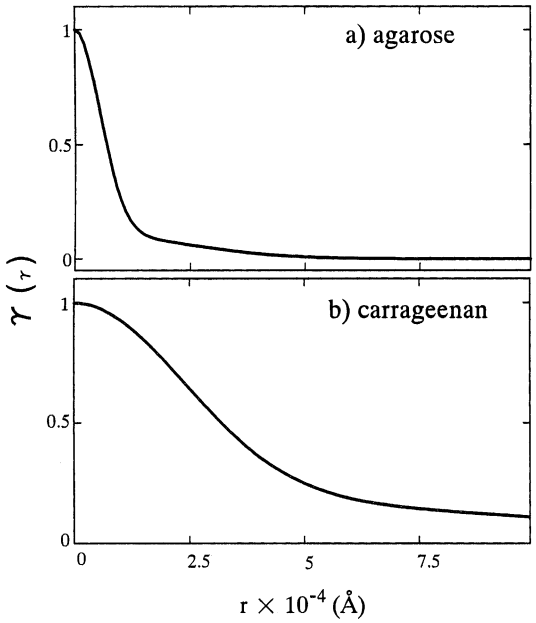

Fig. 11. Recalculated correlation function $\gamma(r)$ against r obtained for the aqueous solutions at 30 °C; (a) agarose; (b) κ-carrageenan.

b are much longer. This indicates that the agarose gel is related to the formation of cross-linking points appeared in polymer-rich phase due to concentration fluctuation of solution, while the gelation of the κ-carrageenan gels, the cross-linking points with a random distribution in solution. Incidentally, $\gamma(r)$ curves of κ-carrageenan gels with 1.5–3% concentrations are the same profile. Accordingly, it may be concluded that the gelation mechanism is quite different in spite of small difference of chemical structure between agarose and κ-carrageenan.

The gelation of carrageenan and agarose solutions has been thought to be due to the coil–helix transition to form network cross-links. Especially, a model concerning stiff gel structure of carrageenan has been proposed as aggregation of double helix structures connected by cations, since the existence of cations plays an important role to reduce electrostatic repulsion between OSO_3 groups [22]. Nevertheless, the aggregation size has never been analyzed. At least, the polarized light scattering experiments provided one concept that the aggregation of the cross-linking junction points takes a random distribution in the solution and the aggregation size is much smaller than the wavelength of He–Ne gas laser to form an uniform structure. For agarose gels, the double helix chains with cross-linking points were performed in the polymer-rich phase. An increase in the helix chains promote the formation of optically anisotropic rods and the gel becomes stiffer with time.

Finally, we shall refer to the properties of air-dried films of agarose and κ-carrageenan prepared by evaporating solvents from gels in a Petri dish, since the gelation mechanisms of the both polymers are quite different in spite of similar chemical structures. Fig. 12 shows X-ray diffraction patterns (end view). The crystallization occurred

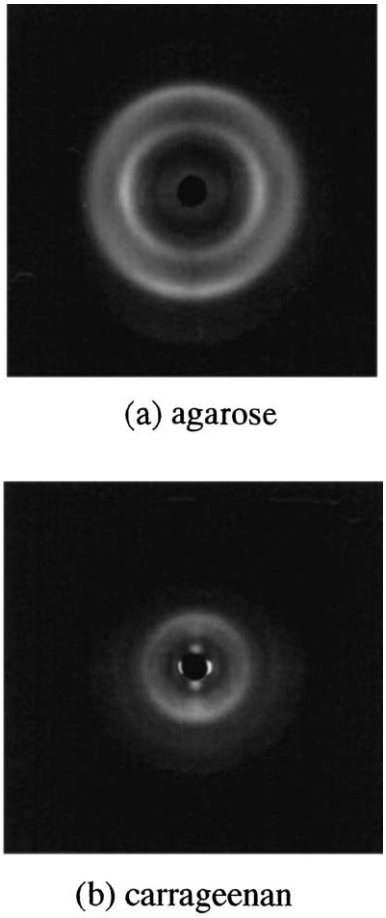

Fig. 12. WAXD patterns (end view) of agarose and κ-carrageenan films.

under the evaporation process of solvent. It is seen that the crystal structures of agarose and κ-carrageenan are quite different but each particular crystal plane of the two polymers orients parallel to the film surface. The preferential orientation parallel to the film surface is thought to be due to the slippage of the crystal plane with highest atomic density by the planner tension. This is due to the strong tension arising parallel to the films surface under the drying condition. The strong tension arise by adhesion between gel and the glass plate, as has been observed for dry gel PVA films [23]. This means that the growth of crystallites of the resultant films is hardly affected by the difference of the gelation mechanisms. The further interest is the difference between mechanical properties of both the films. The appearance of crystallites by evaporating solvents from gels obviously indicates the existence of quasi-crystallites as cross-liking points in gels, although X-ray and DSC cannot detect the existence because of large fluctuation of lattice distance.

Fig. 13 shows the temperature dependence of the storage and loss moduli for the agarose and κ-carrageenan films. The storage modulus E' similar to Young's modulus decreases drastically with increasing temperature but at 40 °C the magnitude of E' increases and decreases again. The increase in the magnitude suggests rubber elasticity due to an increase in molecular mobility of polymer chains at

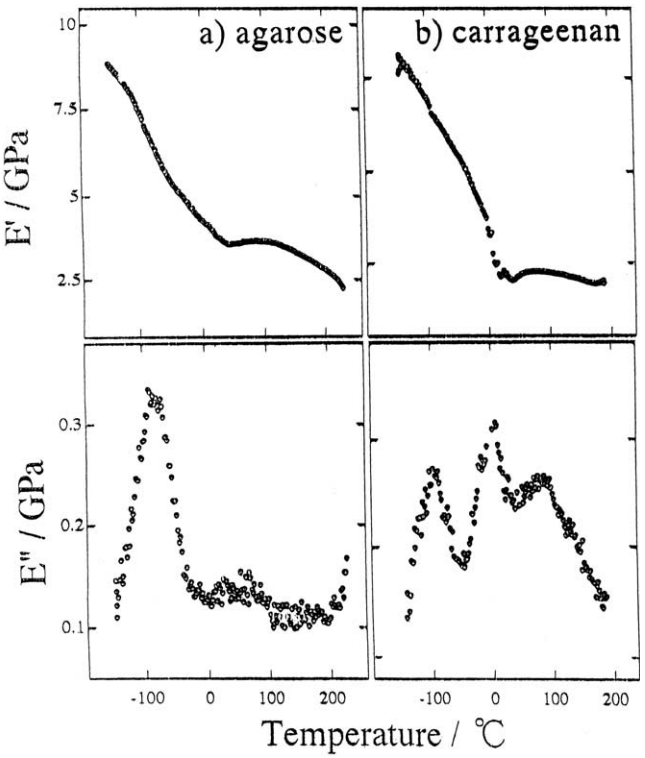

Fig. 13. Temperature dependence of the storage and loss moduli of agarose and κ-carrageenan films.

elevated temperature by the existence of small amount of water which plays as a plasticizer. The corresponding loss modulus E'' shows two dispersion peaks at −80 and 60 °C, respectively, for the agarose film and three peaks at −100, 0 and 95 °C, respectively, for κ-carrageenan film. The peak of E'' at the lowest temperature is probably associated with the local dispersion concerning motion of side groups, while the peak at 0 °C of κ-carrageenan is associated with large motion of amorphous chain segments. The indistinct peak at 60 °C for the agarose film and that at 95 °C of the κ-carrageenan film are thought to be due to the crystal dispersion. Anyway, it turns out that the mechanical relaxations between agarose and κ-carrageenan films are quite different and the Young's modulus of κ-carrageenan film is higher than that of agarose.

Unfortunately, it was very difficult to estimate molecular weights of the agarose and κ-carrageenan. Certainly, the gelation rate and mechanical properties were reported to be sensitive to the molecular weights. Even so, the difference of the gelation mechanisms between agarose and κ-carrageenan solutions is thought to be independent of the molecular weights, as has been confirmed for the gelation of PVA solutions with different molecular weights and tacticity [10].

4. Conclusion

The gelation mechanism of agarose and κ-carrageenan aqueous solutions was investigated by using elastic light scattering techniques in terms of the phase separation due to concentration fluctuation of the solution. The logarithm of scattered intensity from agarose solution increased linearly with time in the initial stage of the liquid–liquid phase separation, when the solutions was quenched in water at constant temperature. If this phenomenon could be analyzed within the framework of the linear theory of spinodal decomposition proposed by Cahn, the phase diagram indicated that the gelation is attributed to the phase separation. Namely, agarose solutions at elevated temperature are thermodynamically unstable at the gelation temperature and tend to incur phase separation. In such supercooled solutions, compact molecular aggregates may be formed and these connect to the heterogeneous network system (polymer-rich phase). In spite of the ordering of molecules in the polymer-rich phase, the behavior does not cause crystallization like polyethylene and polypropylene gels. However, it is evident that there exist quasi-crystallites with such large fluctuation of lattice distance that cannot be detected by X-ray diffraction and DSC measurements. The ordering structure in the polymer-rich phase, however, forms optically anisotropic rods that are independent of crystallization. Such behavior was confirmed by SALS pattern showing a X-type. In contrast, gelation of κ-carrageenan solution is independent of the phase separation of solution. The logarithm of scattered intensity against time showed a constant value indicating gelation due to the rapid formation of cross-linking junction points by coil–helix transition. With the further lapse of time, it is evident that the number of cross-linking points increases and the gel becomes stiffer.

References

[1] Rees DA. Pure Appl Chem 1981;53:1.
[2] Plashchina IG, Muratalieva IR, Braudo EE, Tolstoguzov VB, Morris VJ, Chilvers GR. Carbohydr Polym 1983;3:129.
[3] Watase M, Nishinari K. Food Hydrocolloids 1986;1:25.
[4] Watase M, Nishinari K. Carbohydr Polym 1989;11:55.
[5] Rochas C, Rinaudo M, Landry S. Carbohydr Polym 1990;12:255.
[6] Pines E, Prins W. Macromolecules 1973;6:888.
[7] Feke GT, Prins W. Macromolecules 1975;7:527.
[8] Nishi T, Wang TT, Kwei H. Macromolecules 1975;8:227.
[9] Kanaya T, Ohkura M, Kaji K, Furusaka M, Misawa M. Macromolecules 1994;27:5609.
[10] Matsuo M, Sugiura Y, Takematssu S, Ogita T, Sakabe T, Nakamura R. Polymer 1997;38:5953.
[11] Iida H, Ochi T, Ohashi S, Kohyama K, Nishinari K, Williams P, Phillips GO. In: Nishinari K, Doi E, editors. Food hydrocolloids. New York: Plenum Press; 1994. p. 451.
[12] Matsuo M, Sawatari C, Ohhata T. Macromolecules 1988;21:1317.
[13] Rhodes M, Stein RS. J Polym Sci, Part A-2 1969;7:1539.
[14] Cahn JW. J Chem Phys 1965;42:93.
[15] Cahn JW, Hilliard JE. J Chem Phys 1958;29:258.
[16] Matsuo M, Kawase M, Sugiura Y, Takematsu S, Hara C. Macromolecules 1993;26:4461.

[17] van Aartsen JJ. Eur Polym J 1970;6:919.
[18] Debye P, Chu B, Woermann D. J Chem Phys 1962;36:1803.
[19] Hashimoto T, Kumaki J, Kawai H. Macromolecules 1983;16:641.
[20] Stein RS, Wilson PR. J Appl Phys 1962;33:1914.
[21] Wun KL, Prins W. J Polym Sci, Polym Phys Ed 1974;12:533.
[22] Smidstrod O, Grasdalen H. Carbohydr Polym 1982;2:270.
[23] Sawatari C, Yamamoto Y, Yanagida N, Matsuo M. Polymer 1993;34:95.